Light-Induced Flickering of DsRed Provides Evidence for Distinct and Interconvertible Fluorescent States

Flaminia Malvezzi-Campeggi, Michael Jahnz, Katrin G. Heinze, Petra Dittrich, and Petra Schwille
Experimental Biophysics Group, Max-Planck-Institute for Biophysical Chemistry, D-37077 Göttingen, Germany

ABSTRACT Green fluorescent protein (GFP) from jellyfish *Aequorea victoria*, the powerful genetically encoded tag presently available in a variety of mutants featuring blue to yellow emission, has found a red-emitting counterpart. The recently cloned red fluorescent protein DsRed, isolated from *Discosoma* corals (Matz et al., 1999), with its emission maximum at 583 nm, appears to be the long awaited tool for multi-color applications in fluorescence-based biological research. Studying the emission dynamics of DsRed by fluorescence correlation spectroscopy (FCS), it can be verified that this protein exhibits strong light-dependent flickering similar to what is observed in several yellow-shifted mutants of GFP. FCS data recorded at different intensities and excitation wavelengths suggest that DsRed appears under equilibrated conditions in at minimum three interconvertible states, apparently fluorescent with different excitation and emission properties. Light absorption induces transitions and/or cycling between these states on time scales of several tens to several hundreds of microseconds, dependent on excitation intensity. With increasing intensity, the emission maximum of the static fluorescence continuously shifts to the red, implying that at least one state emitting at longer wavelength is preferably populated at higher light levels. In close resemblance to GFP, this light-induced dynamic behavior implies that the chromophore is subject to conformational rearrangements upon population of the excited state.

INTRODUCTION

After the remarkable breakthrough achieved by the introduction of green fluorescent protein (GFP) as a genetically encoded tag for fluorescence microscopy and spectroscopy on live specimens, there have been tremendous efforts either to find or to design fluorescent proteins with similar properties in the red spectral range for dual- or multicolor applications (Cubitt et al., 1995). Although several different organisms are known to exhibit native fluorescence, it was primarily GFP of jellyfish *Aequorea victoria* that has been subject to a large number of detailed biochemical and biophysical studies as well as design and cloning of a variety of mutants with different photophysical properties (Tsien, 1998). A large palette of enhanced and spectrally shifted mutants has been released to date, with extinction coefficients up to 250,000 M^{-1} cm^{-1} (EGFP) and an emission wavelength range from 450 to 530 nm. However, the goal to find a clonable protein with pronounced red emission near 600 nm had so far not been reached by mutation of jellyfish GFP. Recently, Matz and co-workers (Matz et al., 1999) have succeeded in cloning six new fluorescent proteins from fluorescent but not bioluminescent corals of the Indian and Pacific oceans that appeared to be distant GFP homologs. Of particular importance was a red fluorescent protein that seemed to possess very interesting fluorescence properties, with emission peaking at 583 nm. This protein, drFP5893. or DsRed, is supposed to protect the native organism from the dangerous levels of UV radiation present in strong solar radiation. The light could be absorbed by tryptophans, transferred to the autocatalytically formed chromophore, and then emitted as long-wavelength radiation. According to recent studies of the crystal structure (Wall et al., 2000), the β-barrel secondary structure motif and intrinsic fluorophore show strong similarities to GFP from *Aequorea victoria* (Ormö et al., 1996). An additional oxidation of one backbone bond extends the conjugated π-system of the chromophore and accounts for the red-shifted spectra. It is believed that the oxidation step is accommodated by a rare *cis* configuration of the peptide bond preceding the chromophore and that isomerization around this bond may play a key role in chromophore maturation.

The potential of DsRed as a fluorescent probe in general, and its similarities and differences with respect to GFP in particular, makes an accurate analysis of its spectroscopic properties of great biological interest. The availability of genetically encoded fluorophores in a wavelength range beyond the blue to yellow spectrum is of particular importance for the study of protein-protein interactions and intramolecular protein dynamics, by use of spectrally separable tags for coincidence, cross-correlation, and fluorescence resonance energy transfer (FRET) applications down to the single-molecule level. Consequently, a number of studies have been published recently to elucidate the biochemical and photophysical features of DsRed. Applying confocal one- and two-photon microscopy to EGFP- versus DsRed-expressing *Escherichia coli* cells, Jakobs and coworkers (Jakobs et al., 2000) discuss the use of DsRed for steady-state and time-resolved imaging applications, highlighting a certain ambiguity in its spectral properties that results from long maturation times and the tendency to form aggregates within the expressing organism. A more detailed

Received for publication 7 March 2001 and in final form 6 June 2001.

Address reprint requests to Dr. Petra Schwille, AG Experimentelle Biophysik, Max-Planck-Institut für biophysikalische Chemie, Am Fassberg 11, D-37077 Göttingen, Germany. Tel.: 49-551-2011165; Fax: 49-551-2011435; E-mail: pschwil@gwdg.de.

0006-3495/01/09/1776/10 $2.00

subsequent paper (Baird et al., 2000) corroborates these findings showing that DsRed has indeed a slow and complex kinetics of maturation characterized by a shift from 475-nm excitation/500-nm emission maxima of non-mature protein to 558-nm excitation/585-nm emission maxima typical of mature DsRed. The question about the mechanism that allows the chromophore to have such a maturation process has been faced in an accompanying study (Gross et al., 2000) and was further discussed on the basis of its crystal structure (Wall et al., 2000). Moreover, although the protein is very stable against pH changes, denaturants, and photobleaching (Baird et al., 2000), oligomeric association in solution has been revealed. Even at low concentrations down to the nanomolar regime, DsRed seems to aggregate into at least a tetrameric form in Tris/HCl buffer solution, as shown by slow migration in SDS-polyacrylamide gel electrophoresis, analytical ultracentrifugation, FRET between immature green and mature red DsRed in cells (Baird et al., 2000) as well as by considerably low diffusion coefficients in first fluorescence correlation spectroscopy (FCS) experiments (Heikal et al., 2000).

These previous FCS measurements, which were performed exciting the protein at 488 nm, much below the absorption maximum, reveal a pronounced light-induced flickering process in the low-intensity range of 0.4–7 kW/cm^2 with similar characteristics to those earlier observed for YFP mutants (Schwille et al., 2000; Heikal et al., 2000). Due to this similarity, the conclusion was drawn that in the presence of light, DsRed is cycling between a bright and a dark state with a constant partition fraction. At 488 nm and in the given intensity range, a single characteristic time constant, linearly dependent on intensity, appeared to be sufficient to describe the flickering process. In the present study, also employing the FCS technique on a single-molecule scale, it shall be demonstrated that the photophysical situation gets much more complex near the absorption maximum of DsRed and at higher excitation intensities. The most crucial difference, with respect to the earlier observations, is that more than one of the distinguished spectroscopic states between which the light-induced cycling can be observed is in fact fluorescent. Observing the static fluorescence spectrum of DsRed at different light intensities, a continuous shift toward the red can be seen up to intensities around 40 kW/cm^2, which implies that the flicker-inducing transition process does not involve a fully dark but rather a red-emitting chromophoric state with relatively lower fluorescence efficiency. In addition, a single transition time constant is not sufficient to describe the flicker dynamics at any intensity; instead, two different transition time constants, involving at least three spectroscopically distinguishable states, must be assumed. FCS experiments carried out by dual-color excitation at 543 nm and near-infrared (IR) light at 850 nm, following a scheme proposed by Jung and co-workers (Jung et al., 2000), reveal that the less fluorescent state(s) can in fact be effectively depopulated by the IR line, visible as a drop in the apparent flicker fraction in the FCS curve. Finally, FCS measurements with two-photon excitation well below half the excitation maximum demonstrate that good signal-to-noise ratios are obtainable and that the light-dependent flicker dynamics due to cycling between different states does not play a significant role. This opens up an attractive perspective for in vivo measurements of molecular dynamics of DsRed-tagged proteins.

THEORY

Correlation analysis of fluorescence fluctuations

FCS (Magde et al., 1972; Rigler et al., 1993; Eigen and Rigler, 1994) is a time-averaging fluctuation analysis of small molecular ensembles, combining maximum sensitivity with high statistical confidence. The fluctuations of the fluorescence signal arising from an aqueous solution of fluorescent molecules at a concentration of several nanomolar are analyzed in terms of the normalized fluctuation autocorrelation function $G(\tau)$ defined as:

$$G(\tau) = \frac{\langle \delta F(t)\delta F(t+\tau)\rangle}{\langle F(t)\rangle^2}, \qquad (1)$$

where $F(t) = \langle \mathrm{F}\rangle + \delta F(t)$ is the fluorescence at time t and $\langle F\rangle$ is its mean. In principle, all processes that induce fluctuations of characteristic duration to the measured fluorescence signal can be analyzed by FCS. The simplest form are number fluctuations due to the random motion of freely diffusing molecules through the illuminated volume with lateral and axial dimensions r_0 and z_0, resulting in a diffusion-related expression of the correlation function for particles with characteristic residence time τ_d:

$$G_\mathrm{Diff}(\tau) = (1 + \tau/\tau_\mathrm{d})^{-1}(1 + r_0^2\tau/z_0^2\tau_\mathrm{d})^{-1/2}. \qquad (2)$$

In general, the particles can undergo a multitude of different additional processes that also induce fluctuations in the emission signal and can be easily observed if they occur on faster time scales than the molecular residence time in the volume element τ_d. Assuming that these processes, e.g., reversible inter- or intramolecular reactions, are temporally well separated and that the molecules are slow enough to be considered immobile on the time scale of the fast fluctuations, the overall correlation curve can be approximated by (Palmer and Thompson, 1987; Schwille et al., 2000):

$$G(\tau) = G(0)G_\mathrm{Diff}(\tau)\prod_\mathrm{i} X_\mathrm{i}(\tau), \qquad (3)$$

with $G(0) = N^{-1}$ being the inverse number of molecules in the volume element, and $X_\mathrm{i}(\tau)$ representing the exponential relaxation terms that characterize the reversible transitions between two states of different spectroscopic properties, e.g., different brightness parameters η (defined as the num-

ber of photons collected per single molecule per unit time; see Schwille et al., 1997). In general, the $X_i(\tau)$ have the following functional form:

$$X_i(\tau) = (1 - F_i)^{-1}(1 - F_i + F_i\exp(-\tau/\tau_i)). \quad (4)$$

The relative amplitudes F_i are derived from the average fractions of molecules in the different states, and the transition rates are characterized by the relaxation times τ_i. Since many kinds of simultaneous transitions on different time scales can in principle be observed by FCS, bright and dark (dim) states B and D as well as the associated parameters have to be indexed in a kinetic scheme:

$$(B_i) \underset{k_{b,i}}{\overset{k_{d,i}}{\rightleftarrows}} (D_i)$$

with $\eta_{b,i}$, $\eta_{d,i}$ being the molecular brightness values for states B_i and D_i, respectively, F_i and τ_i can be derived as follows (Palmer and Thompson, 1987):

$$\frac{1}{\tau_i} = k_{d,i} + k_{b,i} \quad (5)$$

$$F = \frac{k_{d,i}k_{b,i}(\eta_{b,i} - \eta_{d,i})^2}{(k_{d,i} + k_{b,i})(k_{b,i}\eta_{b,i}^2 + k_{d,i}\eta_{d,i}^2)} = \frac{k_{d,i}k_{b,i}(1 - \eta_{rel,i})^2}{(k_{d,i} + k_{b,i})(k_{b,i} + k_{d,i}\eta_{rel,i}^2)}, \quad (6)$$

where $\eta_{rel,i} = \eta_{d,i}/\eta_{b,i}$ is the relative brightness of state D_i with respect to state B_i. If one of the states can be considered dark, e.g., state D_i, F_i directly represents the average fraction of molecules in the dark state:

$$F_i = \frac{k_{d,i}}{k_{d,i} + k_{b,i}}. \quad (6a)$$

This relationship was previously found to describe the excitation-induced internal flickering kinetics of several GFP mutants such as EGFP, S65T, and yellow fluorescent proteins in FCS studies (Haupts et al., 1998; Widengren et al.; 1999; Schwille et al., 2000). In some GFP mutants, two different independent transition kinetics ($i = 1, 2$) between at least three different states, two of them being nonfluorescent (dark), could be distinguished (Widengren et al., 1999), whereas the YFP mutant seemed to have only two photophysically distinct states observable by FCS ($i = 1$), one of them assigned as a dark state (Schwille et al., 2000). The observed dynamics appeared to be consistent with the assumption of light-induced conformational substates, e.g., different photoisomers. Since the emission behavior of all these GFP mutants showed strong dependence on pH, internal protonation or deprotonation of the chromophore could also be a likely explanation of the different photophysical properties. In all cases, both the transition toward the bright and to the dark states were found to be light dependent, and a model was established that suggested the first excited state as the strongly favored, if not only, gateway for the bright-dark and the dark-bright transitions (Schwille et al., 2000). Although no saturation of the transition rate could be observed for YFP, and the plot of τ_i^{-1} versus intensity showed basically no deviations from linear behavior in this study, saturation effects for at least the bright-dark transitions were reported for GFP (Widengren at al., 1999) and also have to be taken into account for the present studies on DsRed. In contrast to studies on both GFP and YFP, and also to earlier previous studies on DsRed with excitation well below the absorption maximum (Heikal et al., 2000), the measurements reported here indicate that: 1) there are at least two characteristic time scales on which fluctuations occur, and thus two dynamic processes with $i = 2$ in Eqs. 3–6 have to be assumed; 2) at least two of the three states involved in these processes are fluorescent; and 3) the fractions F_i in Eq. 6, reflecting the contrast of the dynamic effect, are not constant with changing intensity, and thus there is no reason to assume that the transitions $B_i \rightarrow D_i$ and $D_i \rightarrow B_i$ are both dependent on intensity. Rather, the results appear to be consistent with a model assuming the relaxation $D_i \rightarrow B_i$ as spontaneous and independent on excitation light.

MATERIALS AND METHODS

Purification of wild-type DsRed protein

E. coli XL1-Blue cells (Stratagene, Amsterdam, The Netherlands) were transformed by electroporation with pDsRed vector (Clontech, Heidelberg, Germany). Cells were grown to an OD600 of 0.6 in Luria Bertani medium containing 50 μg/ml ampicillin and then induced for 4 h at 37°C with 1 mM isopropyl-β-D-thiogalactoside. The culture was sedimented at 4000 × *g* for 15 min, and the pellet was resuspended in 15 ml of buffer D (20 mM NH_4HCO_3, pH 9.0) before lysis in the French pressure cell. The lysate was centrifuged at 14,000 rpm in a Sorvall SS-34 rotor for 15 min. The supernatant was loaded on an 2- × 4.5-cm Whatman-DE-52 anion-exchange column equilibrated in buffer D, washed with 15 ml of buffer D, and then eluted with a linear 0–500 mM NaCl gradient. DsRed fractions were identified by fluorescence spectroscopy measuring emission at 583 nm using 558-nm excitation wavelength. Samples containing DsRed were pooled, concentrated using Microcon YM-3 spin concentrators (Millipore, Eschborn, Germany), and aliquots were stored at +4°C or −20°C. For measurements, samples were diluted to 10–15 nM in buffer D.

FCS setup and data processing

FCS measurements were performed utilizing a custom-built system in a confocal microscope, as previously described (Schwille et al., 1999, 2000). For excitation, the 488-nm and 514-nm lines of an argon ion laser (Ion Laser Technology, Salt Lake City UT) or a 543-nm helium neon laser (JDS Uniphase, Eindhoven, The Netherlands) were employed. In the dual-color experiment, the 543 HeNe line was superimposed by the continuous ware (cw) line of a tunable titanium-sapphire laser (Tsunami, Spectra Physics, Mountain View, CA). In both cases, the parallel laser beam was focused by a water-immersion objective (Uplan APO 60 × 1.2 W, Olympus, Hamburg, Germany). To obtain large measurement volumes for a good separation of diffusion and fast blinking dynamics, the back aperture was underfilled, resulting in lateral and axial dimensions of $r_0 \approx 1$ μm and z_0

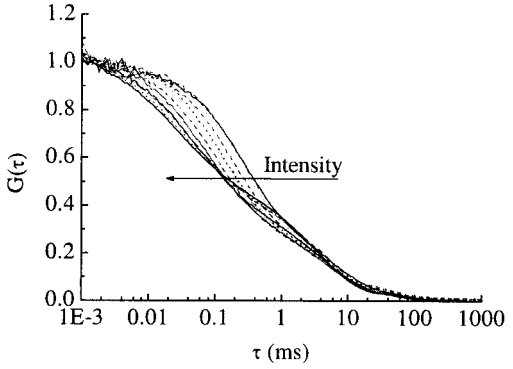

FIGURE 1 Excitation intensity dependence of the normalized autocorrelation curves for DsRed at pH 9, at 543-nm excitation, in the range of 0.5–100 kW/cm^2. The shoulder in the 10-μs to 1-ms time range indicates the fluorescence flickering effect. Two independent time constants can be isolated in this regime, with rates and fractions both strongly dependent on excitation intensity.

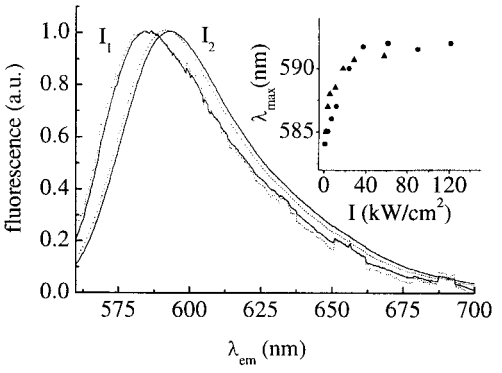

FIGURE 2 Intensity-dependent shift of the static fluorescence spectra for DsRed excited at 488 nm (···) and 543 nm (——). I_1 = 1 kW/cm^2, I_2 = 110 kW/cm^2. The inset marks the behavior of the emission maximum for excitation intensities I_{488} (▲) and I_{543} (●). I_{488} is corrected by a factor of 2 to account for the difference in molecular extinction coefficient at 543 nm.

$\approx$ 4 μm. Fluorescence light was collected through the objective, passing the dichroic mirror and an interference filter (585DF45, AHF Analysentechnik, Tübingen, Germany) and being focused onto a pinhole (50 or 100 μm, interchangeable). The measurements with two-photon excitation were carried out with an IR objective (Uplan APO 60 × 1.2 W IR, Olympus) with 70% transmittance at 950 nm. To discriminate against IR light, an additional 600DF200 bandpass (AHF) filter was used in the dual-color setup. The data collection time varied between 30 and 100 s, depending on the excitation power. The stability of the optical setup, in particular, the size of the measurement volume, was checked routinely with rhodamine-based calibration dyes. The DsRed sample was introduced either as an open droplet or sealed in deep-well slides. The fluorescence signal was autocorrelated over 30–100 s by PC ALV-5000 multiple-τ correlator card (ALV, Langen, Germany). Data manipulation and fitting were performed using ORIGIN software (Microcal, Northampton, MA). Spectra of DsRed and EGFP in the focal measurement volume at different intensities were taken with a fiber-coupled spectrometer (Ocean Optics, Duiven, Netherlands) using an entrance fiber slit of 100 μm.

RESULTS

Intensity-dependent fluorescence of DsRed: evidence of different bright states

Fig. 1 shows the excitation intensity dependence of the normalized correlation curves for DsRed at pH 9, recorded at 543 nm, in the range of 0.5–100 kW/cm^2, in logarithmic steps of factor 0.1 (optical density of neutral glass filters). Similar to results obtained from YFP mutants T203Y and T203F (Schwille et al., 2000), the figure clearly reveals the fast flicker dynamics induced by light. Across the entire range of intensities measured, the diffusion time (τ_d) remained nearly constant ($\sim$2.0 ms) for the whole intensity range with very little photobleaching. On the other hand, the fast decay times τ_i (10 μs to 1 ms), representing the transitions between the bright and dark (or less fluorescent) states, changed with intensity. The absence of a fast-diffusing contaminant was checked by using different pinhole diameters and thus different sizes of the detection volume. Changing the pinhole size from 50 to 100 μm generated an increase in the diffusion time from 1.76 $\pm$ 0.04 ms to 3.72 $\pm$ 0.05 ms, as expected, but the flicker dynamics in the $<$1-ms time scale remained unchanged.

Satisfactory fits of all curves were obtained by using Eq. 3 assuming two characteristic flicker time constants and allowing an additional process in the very fast range to account for triplet-state population and relaxation; i.e., i = 3. However, the triplet dynamics did not contribute significantly to the fit, with time constants τ_3 in the 2-μs regime and a fraction $F_3 < 15\%$ for intensities above 50 kW/cm^2. Triplet-associated dynamics on the microseconds time scale are a common phenomenon for most dyes suitable for FCS (Widengren et al., 1995) and have been found in several GFP mutants (Haupts et al., 1998; Widengren et al., 1999; Schwille et al., 2000). In the observed intensity range, the very fast dynamics thought to be due to triplet-state population did not play a major role and will therefore be omitted for the following discussion. It should be stated, however, that without allowing this dynamic contribution in the time range below 10 μs, the curve fitting was less satisfactory. The slower time range between 10 μs and 1 ms was not sufficiently described by one dynamic process with a single dark state D but instead required the assumption of two internal transition dynamics involving at least three spectroscopically distinguished states of the protein (i.e., B, D_1, and D_2).

To better characterize the emission behavior of the chromophore, the static fluorescence spectra in the focal spot of the FCS setup were recorded at different excitation intensities. The spectra of the mature form of the chromophore, obtained with 488-nm and 543-nm excitation, are reported in Fig. 2. Surprisingly, a red-shift of $\sim$8 nm (from 584 nm to 592 nm) is observed when the intensity is increased from 1 to 110 kW/cm^2. The dependence of the emission maxi-

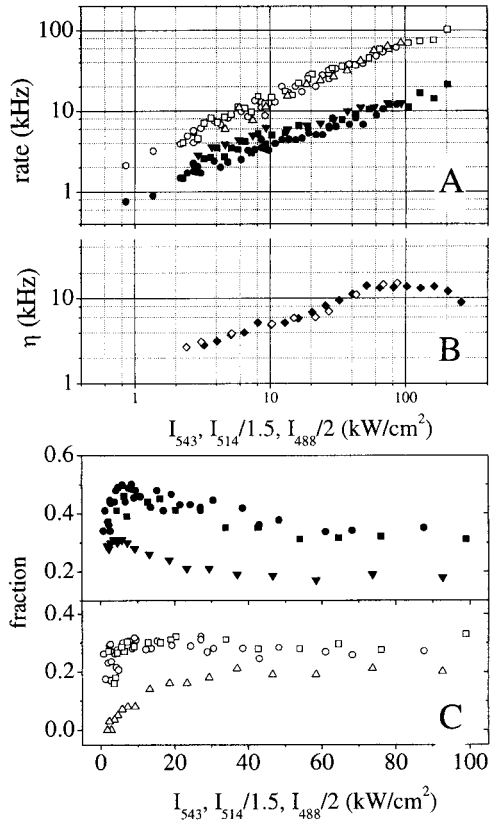

FIGURE 3 (*A*) Intensity dependence of flicker rates for DsRed at pH 9, using 543 nm (○ and ●), 514 nm (□ and ■) and 488 nm (△ and ▲) excitation: τ_1^{-1} (*open symbols*) and τ_2^{-1} (*closed symbols*). (*B*) For comparison, the fluorescence emission rates η (kHz) per molecule, using 543 nm (◇) and 514 nm (◆) excitation. The intensity values at 514 nm and 488 nm are again scaled to account for the difference in molecular extinction coefficient at 543 nm. (*C*) Respective fractions to the above rates τ_i^{-1}: F_1 (*open symbols*) and F_2 (*closed symbols*).

mum on the intensity for the two different excitation wavelengths (see Fig. 2, *inset*) clearly reveals the shift induced by the light. Nevertheless, the maximum value in both cases was achieved at ~40 kW/cm^2 and remained almost constant up to 250 kW/cm^2 (data not shown). It was verified that the observed effect is not introduced by the spectrometer, by carrying out the same kind of measurement with tetramethylrhodamine dye and GFP mutants (EGFP and rsGFP), where no change in the fluorescence spectrum could be found at higher intensities. The light-induced spectral shift in DsRed strongly suggests the presence of at least a second bright state of the chromophore, potentially a different isomer, which is populated via the excited state. When the intensity exceeds 40 kW/cm^2, a constant partition between the states seems to be reached.

As indicated above, the dynamics of two independent flicker processes between states of different fluorescence capacity, in the time regime between 0.01 and 1 ms, were distinguished. Fig. 3 *A* illustrates the intensity dependence of the two relaxation rates τ_1^{-1} and τ_2^{-1}, obtained by fitting the autocorrelation curves with Eq. 3, on two orders of magnitude increase in intensity. For comparison, the overall fluorescence emission rate η at 543 nm and 514 nm, measured in photons per second (kHz) per molecule, were plotted in Fig. 3 *B*. The 488-nm and 514-nm intensity coordinates were scaled by a factor of 0.5 and 0.7, respectively, to account for the different molecular extinction coefficients at 543 nm. As in the case of the YFP mutants (Schwille et al. 2000), a substantial decrease of the τ_i values is obtained at high intensity, but the relaxation rates show a close to linear increase only at excitation intensities of a few kW/cm^2. The flicker rates differ by a factor of ~5 with an increasing discrepancy toward higher intensities.

The values of the respective fractions F_1 and F_2 are plotted in Fig. 3 *C*. Interestingly, F_1 and F_2 show a considerable dependency on excitation intensity for all three excitation wavelengths, which is in contrast to studies on YFP and GFP mutants and also to previous measurements reported on DsRed at 488 nm (Heikal et al., 2000). However, the latter need not be a true contradiction. At very low intensity (<10 kW/cm^2), the correlation curves recorded at 488 nm showed an overall fraction of only ~0.3, which could well be fitted with only one flickering process. In this case, the fraction remained constant within experimental errors, in accordance with the findings by Heikal et al. (2000). Only at higher intensities and where the excitation is closer to the absorption maximum of DsRed was the assumption of only one flicker dynamics not sufficient for proper curve fitting.

All results obtained by static and dynamic fluorescence measurements are compatible with the presence of two light-dependent flickering processes in the range between 0.01 and 1 ms, requiring the introduction at least three spectroscopically distinguishable states of the chromophore, two of which are assumed to be fluorescent to a certain extent. Although the excitation intensity dependence of both rates τ_1^{-1} and τ_2^{-1} can be described as linear for intensities below 10 kW/cm^2, saturation effects resulting in deviations from linear behavior are observed above this value.

FCS diffusion analysis

The diffusion coefficient for DsRed molecules in aqueous solution, determined by FCS in different optical setups, is consistently given by $(3.7 \pm 0.1) \times 10^{-7}$ cm^2/s, more than two times slower than the values determined for GFP in the same environment $(8.7 \pm 0.2) \times 10^{-7}$ cm^2/s. For globular molecules, the diffusion time scales proportional with the cube root of the molecular mass; thus, the diffusing DsRed particles seem to be up to eightfold larger than single GFP units. Because both proteins share about the same number of amino acids, and a similar β-barrel-like topology (Wall et al., 2000), there is indeed reason to assume that DsRed is present at higher aggregates even at nanomolar concentra-

tions. This is consistent with previous biochemical and structural investigations (Baird et al., 2000; Wall et al., 2000) suggesting that DsRed has a high tendency to form tetra- or even octamers. However, the measured values for DsRed diffusion coefficients are larger than those reported in previous FCS measurements (Heikal et al., 2000), and no tendency to form even higher aggregates of precipitates was observed. The different protein purification protocol or buffer conditions chosen in our study could account for the disparity.

pH dependence

The absence of a dark protonated state can be verified through the study of the pH dependence of the fluorescence autocorrelation curves at low excitation intensity (8–9 kW/cm^2). Exciting the sample at 543 nm, 514 nm, and 488 nm, almost no difference is observed in the correlation curves when the pH is varied between 6 and 11 (data not shown). All the curves were satisfactory fitted by Eq. 3 without introduction of a pH-related additional dynamics as required for GFP and YFP mutants. The pH-dependent dark state in GFP mutants was attributed to the protonated state of the chromophore with an absorption band at 390 nm (Haupts et al., 1998). The lack of this band in the case of DsRed already suggested the absence of a protonated form in this protein (Matz et al., 1999) and was previously confirmed by Heikal et al. (2000) through FCS analysis. A compromised signal-to-noise ratio when a pH 5 buffer is used, probably due to aggregation, prevents FCS analysis of DsRed in the low pH range. Nevertheless, nearly 60% of the static fluorescence is preserved at pH 5, whereas a complete loss of the fluorescence signal can be observed at pH 3 (data not shown).

Two-color excitation: depopulation of the dark state(s)

The fact that a red-shifted fluorescent state seems to be increasingly populated at high intensities, as observed in the static fluorescence spectra, suggests that this red-emitting state is also involved in the transition dynamics recorded by FCS. It is likely that both the absorption spectrum and the emission spectrum are changed at high intensities with respect to the low-intensity spectra of DsRed recorded by conventional spectrometers. For that reason, two-color excitation was utilized in FCS measurements, following a scheme proposed by Jung et al. (2000), to reveal the spectroscopic identity of the states involved in the flicker dynamics. If the populated dark or dim states absorb in a shifted spectral range, a properly chosen second exciting laser beam in principle allows one to probe the population of these states, by changing the rates and amplitudes (τ_i and F_i) of the dynamic effects in the correlation curve. In the case of DsRed, the shift in the static fluorescence spectra suggests that at high intensity, the absorption is shifted toward the red. Thus, to test the response of the flicker dynamics to the presence of an additional excitation line in the red spectral range far away from the fundamental excitation, an 850-nm cw laser beam from a titanium-sapphire laser was superimposed with the 543-nm line in the objective's focal point, i.e., the measurement volume. Fig. 4 shows the effect of this superimposed beam: with increasing intensity at 850 nm, the fraction of flicker dynamics as well as the characteristic overall decay time decrease significantly, indicating an effective depopulation of the less fluorescent (red-shifted) state(s) and a faster relaxation back to the fundamental bright state. The average fluorescence signal increased slightly, which rules out the possibility of a general depopulation of the excited states. Due to the decreased overall fraction, fitting the curves with two dynamic processes no longer allows convincing identification of two consistent values for F_1 and F_2, respectively, τ_1 and τ_2. For that reason, average F and τ were determined assuming a single fast dynamic process. Both values drop by ~50% for the highest intensity applied at 850 nm.

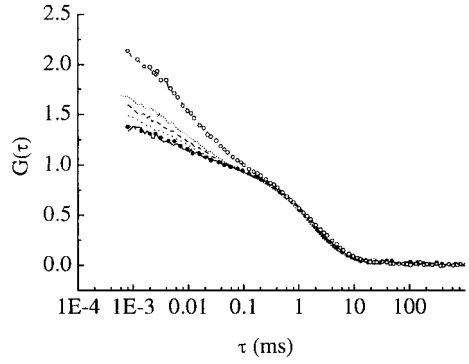

FIGURE 4 Correlation curves of DsRed excited at 543 nm and 130 kW/cm^2, with superimposed IR-light beam. The IR light was tuned to 850 nm; the respective excitation intensity was 0 (○), 1.7 (*small dots*), 2.4 (— — —), 3.1 (· · ·), 3.5 (●), 4.2 (——) $\times 10^3$ kW/cm^2.

Two-photon excited FCS of DsRed

It has been shown previously (Jakobs et al., 2000; Heikal et al., 2000) that DsRed exhibits significant two-photon absorption cross sections when excited well above 900 nm. Since the absorption maximum of two-photon excitation is, as with many other dyes previously investigated (Xu et al. 1996; Schwille et al., 1999), blue-shifted with respect to the one-photon spectra, two-photon excitation allows us to probe the photophysical dynamics by FCS in a wavelength regime that is far away from the fundamental transition. From the wavelength dependence of the one-photon correlation curves, it could already be verified that the fast dynamic effect gets less pronounced and the fractions F_i

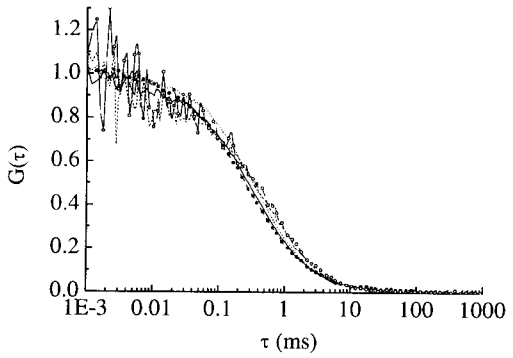

FIGURE 5 Normalized correlation curves for DsRed obtained by two-photon excitation. The sample is illuminated with 100-fs pulses, 80 MHz, at 950 nm. The beam diameter at the back aperture of the objective is 8.0 mm. The reported curves refer to excitation levels of 38 mW (●), 30 mW (——), 24 mW (· · ·), 10 mW (— — —), and 6 mW (○) and show no intensity dependence of the fast time range under these conditions.

decrease with increasing distance from the absorption maximum (see Fig. 3 *C*). If DsRed is two-photon excited at 950 nm (100 fs, 80 MHz pulsed excitation, in contrast to the two-color studies described above), no fast flicker effect could be identified with changes in intensity (Fig. 5). There is only a slight decrease in diffusion times at high intensities, most likely due to photobleaching. The obtained emission yield η is sufficiently high at this wavelength, ranging from 1.2 to 11.5 kHz/molecule in the observed intensity range. This fact as well as the eliminated internal dynamics promises an interesting perspective for the employment of DsRed as a genetically encoded tag for intracellular FCS measurements.

DISCUSSION

Fig. 6 depicts the working model underlying the data evaluation of the fast kinetics of DsRed as observed by FCS. Excitation of the molecule in its native fluorescent state B allows transitions between B and two states D_1 and D_2 that possess different spectroscopic properties. The rates of these transitions, $k_{d,1}$ and $k_{d,2}$, are dependent on intensity but clearly exhibit saturation. Based on their measured dynamics, it is not possible to distinguish between a competitive and a parallel mechanism of D_1 and D_2 population via B. However, because the time scales of transition dynamics $B \rightarrow D_1$ and $B \rightarrow D_2$ differ by a factor of 5 over a large intensity range, the processes are for simplicity's sake considered independent. Although this closely resembles earlier photophysical models for GFP (Widengren et al., 1999) and YFP mutants (Schwille et al., 2000), the relaxation rates back from D_1 and D_2 are not intensity dependent in the case of DsRed. Instead, to properly describe the intensity dependence of the fractions F_1 and F_2, the backward rates $k_{b,1}$ and $k_{b,2}$ are assumed to be spontaneous for excitation at 543 nm and below. Because the relaxation of the excited states takes place on a nanoseconds time scale, much faster than the observed relaxation kinetics between states B and D_i, there is no need to differentiate between their ground and excited states in the overall kinetic model.

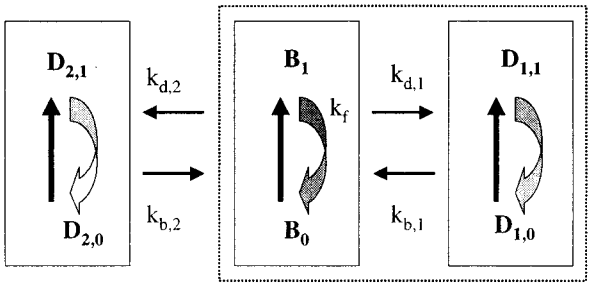

FIGURE 6 Proposed model to describe the intramolecular dynamics in DsRed as described above. The fast flickering is thought to involve at least three different interconvertible (fluorescent) states. Population of D_1 and D_2 obviously occurs via the excited state of B; the relaxation back to B is in both cases spontaneous but can be enhanced if IR light is superimposed to the fundamental excitation line.

To explain the obvious intensity dependence of flicker rates and fractions, the transitions to the respective dark, or less fluorescent, states D_i are for both dynamics assumed to occur via the first excited fundamental state B. The overall transition rate $k_{d,i}$ is dependent on both the excited-state population and the transition rate from the excited state, or crossing rate, $k_{cd,i}$. On the other hand, the excited-state population depends on the intensity, I_{ex}, the excitation cross section in state B, σ_b, and the fluorescence decay rate k_{fb}. It is assumed that saturation plays a crucial role at high intensities; thus, the expression for $k_{d,i}$ reads:

$$k_{d,i} = k_{cd,i}\frac{\sigma_b I_{ex}}{\sigma_b I_{ex} + k_{fb}}. \tag{7}$$

The relaxation back to the fundamental state B at the applied excitation wavelengths is considered to be spontaneous, i.e., not dependent on intensity, and occurs with the respective rates $k_{b,i}$. The characteristic relaxation constant τ_i for transition i is then given by:

$$\tau_i = \left(k_{cd,i}\frac{I_{ex}}{I_{ex} + k_{fb}/\sigma_b} + k_{b,i}\right)^{-1}. \tag{8}$$

With the fractions defined by the forward and reverse rates as in Eq. 6, the following expressions are obtained for describing the intensity-dependent experimental data $\tau_i(I_{ex})$ and $F_i(I_{ex})$ in Fig. 3:

$$\frac{1}{\tau_i}(I_{ex}) = \frac{p_{1,i}}{1 + p_{2,i}/I_{ex}} + p_{3,i} \tag{9a}$$

$$F_i(I_{ex}) = \frac{(p_{4,i} + p_{5,i}/I_{ex})(1 - \eta_{rel,i})^2}{(1 + p_{4,i} + p_{5,i}/I_{ex})(\eta_{rel,i}^2 + p_{4,i} + p_{5,i}/I_{ex})}, \tag{9b}$$

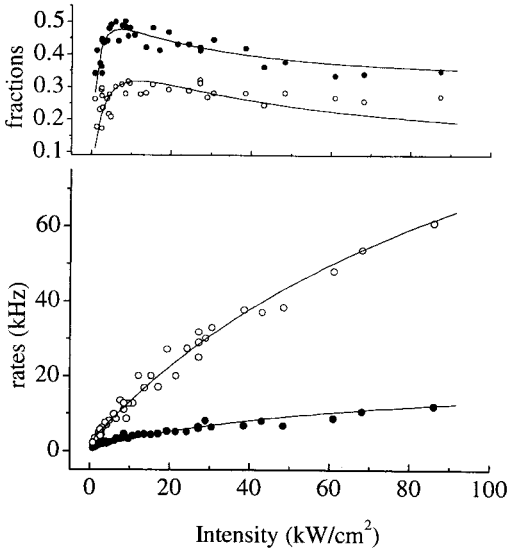

FIGURE 7 Fractions (*upper panel*), i.e., F_1 (○) and F_2 (●), and rates (*lower panel*), i.e., $1/\tau_1$ (○) and $1/\tau_2$ (●), versus excitation intensity, for DsRed at pH 9, using 543-nm excitation. The lines represent the best fit obtained by using Eqs. 9; the fitting parameters are summarized in Table 1.

where the parameters p are given as follows: $p_{1,i} = k_{cd,i}$; $p_{2,i} = k_{fb}/\sigma_b$; $p_{3,i} = k_{b,i}$; $p_{4,i} = p_{3,i}/p_{1,i}$; and $p_{5,i} = p_{2,i}p_{4,i}$. Since the static fluorescence measurements suggest that at least two of the states populated at the applied intensities are fluorescent, the relative detection efficiencies $\eta_{rel,1}$ and $\eta_{rel,2}$ for the states D_1 and D_2 with respect to state B must be included in the expression of the fractions. Strictly, $p_{2,i}$, representing the theoretical saturation intensity of state B if no competitive processes are present, should not be indexed because both transitions $B \rightarrow D_1$ and $B \rightarrow D_2$ involve the same fundamental state B. On the other hand, because both dynamics are thought to be uncoupled, and the transition to D1 is occurring at a much faster rate than the other one, the transition toward D_2 will always involve a state mixture of both, B and D_1; thus, the effective value for $p_{2,2}$ will be different from $p_{2,1}$. The values obtained by simultaneously fitting both data series, flickering rates and fractions for excitation at 543 nm (Fig. 7), are listed in Table 1. The plots for the obtained values (fitting curves) are included in Fig. 7 and show a good agreement with the experimental data. At very high intensity (>50 kW/cm^2), the separation of different time scales is more difficult, because the above mentioned fractions and rates for the fast triplet dynamics (not plotted) can no longer be separated easily. This causes difficulties in determining the exact values for F_i, which can be verified by the stronger deviation of the fitting function from the measured data in the high-intensity regime (Fig. 7). The forward rate constants toward D_1 and D_2, given by $p_{1,i}$, differ by a factor of 7, whereas the backward rates $p_{3,i}$ are different by a factor of only 3. The saturation intensity $p_{2,i}$ for the fundamental state B is 110 kW/cm^2, as determined from the fast transition, and 70 kW/cm^2, as determined from the slow transition. As indicated above, these values differ due to a mixture of states involved in the slow transition. Both values are by a factor of 2–3 larger than the apparent saturation intensity of 30 kW/cm^2 previously reported by Heikal et al. (2000). However, the value of $\sim 3 \times 10^{23}$ photons/cm^2 s is still considerably smaller than the theoretical value 2×10^{24} photons/cm^2 s, as determined from the fluorescence decay rate k_{fb} and the absorption cross-section σ_b (Heikal et al., 2000). The evaluation of FCS data furthermore suggests that both states D_i exhibit residual fluorescence, ~28% for D_1 and ~18% for D_2.

TABLE 1 Parameters of the best-fit curves for both the flickering rates τ_i^{-1} and fractions F_i of the observed intermolecular dynamics in DsRed, excited at 543 nm

Parameters	State D_2 (slow transition)	State D_1 (fast transition)
p_1 (kHz) (forward rate)	22 ± 3	140 ± 10
p_2 (kW/cm^2) (saturation intensity)	70 ± 10	110 ± 10
p_3 (kHz) (backward rate)	0.65 ± 0.05	2.0 ± 0.6
η_{rel} (relative emission yield)	0.18 ± 0.01	0.28 ± 0.01

The parameters p_1, p_2, p_3, and η_{rel} refer to Eqs. 9 in the text.

If IR at 850 nm is superimposed with the excitation line at 543 nm, the obvious decrease (Fig. 4) of the fractions F_i and the characteristic time constants τ_i indicates that the additional illumination source can effectively depopulate at least one of the two less fluorescent, spectrally distinguishable, states D_1 and D_2. This agrees with the static fluorescence observation, suggesting that the overall spectra are at any time a mixture between the fundamental bright state and a red-shifted state, the fraction of which increases with increasing intensity. In a simplified model, it is assumed that the back transition rates from states D_1 and/or D_2 under IR excitation, $k_{xb,i}$, are no longer spontaneous but enhanced by an additional pathway via the excited state, i.e., linearly dependent on the intensity I_2 of the superimposed IR light:

$$k_{xb,i} = k_{b,i} + \sigma_{eff,i} I_2. \quad (10)$$

As pointed out, the dramatic decrease in the fractions induced by IR illumination allows us to no longer unequivocally fit two distinct values for fractions and time constants; therefore, only an estimation can be given for $\sigma_{eff,i}$ as an average parameter. By fitting the curves by an overall rate and fraction, according to Eqs. 9 and 10, the effective transition cross section $\sigma_{eff,i}$ toward B upon excitation at 850 nm is ~5 Hz/(kW/cm^2) as determined by an increase of the average flicker rate τ_f^{-1} by 20 kHz at 4×10^3 kW/cm^2.

Conclusions and outlook

Measurements of the red fluorescent protein DsRed by FCS reveal the presence of a strong light-induced flickering

phenomenon in the time range from tens to hundreds of microseconds. A detailed analysis of the correlation curves in this time regime shows that at least two characteristic time constants can be isolated, in addition to the diffusion time constant given by the molecule's residence in the measurement volume and a very fast process (microseconds) at high intensities, presumably due to intersystem crossing to the triplet state. The strong intensity dependence of these two flickering processes indicates that the first excited state of DsRed in its basic fluorescent form B appears to act as a gateway to, at least, two other spectroscopically distinct molecular states, D_1 and D_2, of the protein. Moreover, a pronounced light-induced shift in the emission maximum of the static fluorescence spectra strongly suggests that at least one of these states, preferably populated at high intensities, is fluorescent itself. The average fluorescence emission rate per molecule, fluorescence quantum yield, and overall photon collection efficiency of the optical setup (~1%) can provide an estimate of the transition quantum yield to D_1 and D_2. For every excitation process, a chance of ~2% (0.3%) exists for transition to D_1 (D_2). Although both states appear to be fluorescent to a certain extent (Table 1), the transition back to B does not seem to involve the excited state but occurs with a spontaneous rate of 2 kHz (0.65 kHz). However, illumination of the system by IR allows for efficient depopulation of at least one of the states D_i. Increasing intensity of this second illumination source continuously diminishes the contrast of fast dynamics, or fractions F_i, in the correlation curves and accelerates the transition kinetics. Although the pathway of relaxation back to the B state cannot be revealed by this method, the requirement of a rather long wavelength to depopulate D_i suggests that higher excited states, or even triplet states, are involved. However, the possibility that one of the distinguished dim states D_1 and D_2 is, due to its spontaneous relaxation characteristics, a triplet state itself, seems highly unlikely. As mentioned in the results section, a fast effect in the microseconds time scale has been observed at high intensities in addition to the B-D_1 and B-D_2 dynamics, which is far more probable to involve a true triplet excited state. In addition to that, the determined relative brightness values of $\eta_{rel,1}$ and $\eta_{rel,2}$ of 0.28 and 0.18, respectively, for D_1 and D_2, are far higher than would be expected for phosphorescence.

Although from our dynamic analysis nothing can be concluded about the structural identities of D_1 and D_2, the time scales of the observed dynamics are, in accordance with dynamic effects in other fluorescent proteins, consistent with conformational rearrangements of the chromophoric unit, e.g., light-induced isomerization processes (Widengren et al., 1999; Schwille et al., 2000; Widengren and Schwille, 2000). Previously, Matz et al. (1999) observed the presence of a single absorption band in DsRed, analogous to the 480-nm band of GFP, suggesting that the fluorophore is always unprotonated. FCS experiments performed at different pH values support this view by revealing no changes in the fast regime of the autocorrelation curves. It is therefore unlikely that proton shuttling to and from the chromophore plays an important role in the observed dynamics. In comparison to the flickering phenomenon of GFP mutants and YFPs, DsRed shows a striking increase of overall fractions of the light-induced fast blinking effects as the excitation/emission spectra are shifted toward the red. Found to be ~15% in EGFP (Haupts et al., 1998) and 50% in YFP (Schwille et al., 2000), the fractions approach 60–70% in DsRed, whereas the characteristic time constants always stay well within the range of 10 μs to 1 ms. Since efforts are underway to enhance the spectral palette of fluorescent proteins to emission wavelengths above 600 nm (Baird et al., 2000), it will be interesting to see whether this tendency gets corroborated. To reveal the true spectral identity and energy levels of the at least three distinguished chromophoric states of DsRed, high-resolution spectroscopy and spectral hole-burning on this protein, analogous to the studies published on GFP mutants (Creemers et al., 2000), remains an important task. Another crucial question to be addressed is whether and how the presence of DsRed as a multimer, probably composed of heterogeneous (mature and immature) chromophoric units, affects the dynamics described above. Recent studies on single immobilized oligomeric units of DsRed (Cotlet et al., 2001) report collective effects in chromophore emission represented by discrete steps of the measured count rates, which are likely due to energy transfer within the proposed tetramers. To answer this question, e.g., to test whether intervals of collective emission relate to the different fluorescent forms B, D_1, and D_2 identified here, the availability of monomeric DsRed mutants for comparative spectroscopic analysis would be highly desirable.

An exciting perspective is opened up by the two-photon FCS results obtained with DsRed. With a count rate per molecule and second of $\eta \approx 12$ kHz, the obtainable signal quality is almost as high as in one-photon measurements close to the excitation maximum in much larger measurement volumes ($\eta \approx 17$ kHz). As previously reported, maximum two-photon detection yields of certain dyes can differ significantly from the one-photon counterparts in idealized setups (Schwille et al., 1999); in the case of several rhodamines, the difference was found to be as high as a factor of 5–7, most likely due to enhanced photobleaching or population of higher excited states. However, DsRed seems to be a remarkably stable dye under two-photon conditions. Even at very high power levels above 30 mW, no significant shortening of diffusion times, a sensitive indicator for dynamic photobleaching (Widengren and Rigler, 1997), could be observed. Additionally, the light-induced flickering clearly visible for one-photon excitation can be efficiently suppressed. This might be a consequence of greatly overlapping two-photon absorption cross sections for the different identified fluorescent substates. The fact that many

different chromophores can be equally well excited at common IR wavelengths has recently enabled us to simultaneously two-photon excite even spectrally separable dyes in the green and red emission range (Heinze et al., 2000). The results reported here suggest that DsRed has the potential to be a superb genetically encoded tag for intracellular measurements with maximum sensitivity, once the unfortunate properties of slow maturation and aggregation are corrected by means of slightly modified mutants.

We thank Kirsten Bacia, Elke Haustein, and Andre Koltermann for helpful discussions, Karin Birkenfeld for assistance with sample preparation, and Sally Kim for proofreading the manuscript.

Financial support by the German Ministry for Education and Research (Biofuture grant 0311845) and Evotec OAI, Hamburg, Germany, is gratefully acknowledged. F.M.C. was supported by a fellowship by the Italian Ministry for University and Scientific Research.

REFERENCES

Baird, G. S., D. A. Zacharias, and R. Y. Tsien. 2000. Biochemistry, mutagenesis, and oligomerization of DsRed, a red fluorescent protein from coral. *Proc. Natl. Acad. Sci. U.S.A.* 97:11984–11989.

Cotlet, M., J. Hofkens, F. Köhn, J. Michiels, G. Dirix, M. Van Guyse, J. Vanderleyden, and F. C. De Schryver. 2001. Collective effects in individual oligomers of the red fluorescent coral protein DsRed. *Chem. Phys. Lett.* 336:415–423.

Creemers, T. M. H., A. J. Lock, V. Subramaniam, T. M. Jovin, and S. Völker. 2000. Photophysics and optical switching in green fluorescent protein mutants. *Proc. Natl. Acad. Sci. U.S.A.* 97:2974–2978.

Cubitt, A. B., S. R. Heim, A. E. Adams, A. E. Boyd, L. A. Gross, and R. Y. Tsien. 1995. Understanding, improving and using green fluorescent proteins. *Trends Biochem. Sci.* 20:448–455.

Eigen, M., and R. Rigler. 1994. Sorting single molecules: applications to diagnostics and evolutionary biotechnology. *Proc. Natl. Acad. Sci. U.S.A.* 91:5740–5747.

Gross, L. A., G. S. Baird, R. C. Hoffman, K. K. Baldridge, and R. Y. Tsien. 2000. The structure of the chromophore within DsRed, a red fluorescent protein from coral. *Proc. Natl. Acad. Sci. U.S.A.* 97:11990–11995.

Haupts, U., S. Maiti, P. Schwille, and W. W. Webb. 1998. Dynamics of fluorescence fluctuations in green fluorescent protein observed by fluorescence correlation spectroscopy. *Proc. Natl. Acad. Sci. U.S.A.* 95: 13573–13578.

Heikal, A. A., S. T. Hess, G. S. Baird, R.Y. Tsien, and W. W. Webb. 2000. Molecular spectroscopy and dynamics of intrinsically fluorescent proteins: coral red (dsRed) and yellow (citrine). *Proc. Natl. Acad. Sci. U.S.A.* 97:11996–12001.

Heinze, K. G., A. Koltermann, and P. Schwille. 2000. Simultaneous two-photon excitation of distinct labels for dual-color fluorescence cross-correlation analysis. *Proc. Natl. Acad. Sci. U.S.A.* 97: 10377–10382.

Jakobs, S., V. Subramaniam, A. Schönle, T. M. Jovin, and S. W. Hell. 2000. EGFP and DsRed expressing cultures of *Escherichia coli* imaged by confocal, two-photon and fluorescence lifetime microscopy. *FEBS Lett.* 479:131–135.

Jung, G., S. Mais, A. Zumbusch, and C. Bräuchle. 2000. The role of dark states in the photodynamics of the green fluorescent protein examined with two-color fluorescence excitation spectroscopy. *J. Phys. Chem.* 104:873–877.

Magde, D., E. L. Elson, and W. W. Webb. 1972. Thermodynamic fluctuations in a reacting system - measurement by fluorescence correlation spectroscopy. *Phys. Rev. Lett.* 29:705–708.

Matz, M. V., A. F. Fradkov, Y. A. Labas, A. P. Savitsky, A. G. Zaraisky, M. L. Markelov, and S. A. Lukyanov. 1999. Fluorescent proteins from nonbioluminescent *Anthozoa* species. *Nat. Biotechnol.* 17:969–973.

Ormö, M., A. B. Cubitt, K. Kallio, L. A. Gross, R. Y. Tsien, and S. J. Remington. 1996. Crystal structure of the *Aequorea victoria* green fluorescent protein. *Science.* 273:1392–1395.

Palmer, A. G., and N. L. Thompson. 1987. Theory of sample translation in fluorescence correlation spectroscopy. *Biophys. J.* 51:339–343.

Rigler, R., Ü. Mets, J. Widengren, and P. Kask. 1993. Fluorescence correlation spectroscopy with high count rates and low background: analysis of translational diffusion. *Eur. Biophys. J.* 22:169–175.

Schwille, P., U. Haupts, S. Maiti, and W. W. Webb. 1999. Molecular dynamics in living cells observed by fluorescence correlation spectroscopy with one- and two-photon excitation. *Biophys. J.* 77:2251–2265.

Schwille, P., S. Kummer, A. A. Heikal, W. E. Moerner, and W. W. Webb. 2000. Fluorescence correlation spectroscopy reveals fast optical excitation-driven intramolecular dynamics of yellow fluorescent proteins. *Proc. Natl. Acad. Sci. U.S.A.* 97:151–156.

Schwille, P., F.-J. Meyer-Almes, and R. Rigler. 1997. Dual-color fluorescence cross-correlation spectroscopy for multicomponent diffusional analysis in solution. *Biophys. J.* 72:1878–1886.

Tsien, R. Y. 1998. The green fluorescent protein. *Annu. Rev. Biochem.* 67:509–544.

Wall, M. A., M. Socolich, and R. Ranganathan. 2000. The structural basis for red fluorescence in the tetrameric GFP homolog DsRed. *Nat. Struct. Biol.* 7:1133–1138.

Widengren, J., Ü. Mets, and R. Rigler. 1995. Fluorescence correlation spectroscopy of triplet states in solution: a theoretical and experimental study. *J. Chem. Phys.* 99:13368–13379.

Widengren, J., Ü. Mets, and R. Rigler. 1999. Photodynamic properties of green fluorescent proteins investigated by fluorescence correlation spectroscopy. *Chem. Phys.* 250:171–186.

Widengren, J., and R. Rigler. 1996. Mechanisms of photobleaching investigated by fluorescence correlation spectroscopy. *Bioimaging.* 4:149–157.

Widengren, J., and P. Schwille. 2000. Characterization of photo-induced isomerization and back-isomerization of the cyanine dye Cy5 by fluorescence correlation spectroscopy. *J. Phys. Chem.* 104:6416–6428.

Xu, C., W. Zipfel, J. B. Shear, R. M. Williams, and W. W. Webb. 1996. Multiphoton fluorescence excitation: new spectral windows for biological nonlinear microscopy *Proc. Natl. Acad. Sci. U.S.A.* 93: 10763–10768.